Journal of Crystal Growth 384 (2013) 82–87

Contents lists available at ScienceDirect

Journal of Crystal Growth

journal homepage: www.elsevier.com/locate/jcrysgro

Growth of InAs quantum dots on Si-based GaAs nanowires by controlling the surface adatom diffusion

Xin Yan, Xia Zhang *, Junshuai Li, Jiangong Cui, Qi Wang, Yongqing Huang, Xiaomin Ren

State Key Laboratory of Information Photonics and Optical Communications, Beijing University of Posts and Telecommunications, Beijing 100876, China

ARTICLE INFO

Article history:
Received 17 June 2013
Received in revised form
26 August 2013
Accepted 12 September 2013
Communicated by: K. Deppert
Available online 20 September 2013

Keywords:
A1. Nanostructures
A3. Metalorganic chemical vapor deposition
B1. Nanomaterials
B2. Semiconducting III–V materials
B2. Semiconducting silicon

ABSTRACT

InAs/GaAs dots-on-nanowire (NW) hybrid heterostructures are grown on Si substrate by metal organic chemical vapor deposition. The formation of InAs quantum dots (QDs) is intimately associated with the NW density as well as the substrate surface properties, both of which strongly affect the surface adatom diffusion. InAs QDs are realized with a short deposition time by reducing the NW density. The QDs exhibit specific facets and pure zinc blende structure, residing on a wetting layer of several nanometers. Photoluminescence emission from the QDs is observed at room temperature, with a linewidth of 186 meV. The results are promising for future integration of III–V NW hybrid devices, especially photovoltaic cells on Si.

1. Introduction

III–V semiconductor nanowires (NWs) have attracted great attention for their potential in future optoelectronic devices such as lasers, solar cells and light emitting diodes (LEDs) [1–3]. Due to the particular geometry, NWs can be used to fabricate various heterostructures, e.g. axial and core–shell structures, which is beneficial for achieving devices with multiple functions and high performance [1,4]. A promising NW heterostructure is a hybrid combination of NWs and quantum dots (QDs), which integrates excellent optical properties with waveguiding and optical cavity functions [5,6]. Compared with the widely studied QD-in-NW structure [7,8], QDs-on-NW structure is expected to have a much higher gain and broader linewidth, which is promising in future solar cells and LEDs [9–12]. QDs-on-NW structures have been realized in several material pairs, including Ge QDs on Si NWs, MnAs QDs on InAs NWs, InAs QDs on InP NWs and In(Ga)As QDs on GaAs NWs [9–16]. Particularly, In(Ga)As QDs formed on GaAs NWs exhibit high crystal quality and excellent optical properties [9,12,16,17]. However, up to now, most of the studies only focus on the QDs, isolated from the NWs and substrate, although both of which are believed to have a great influence on the formation of QDs due to adatom diffusion mechanism [12,15].

Integrating III–V NW structures on Si has attracted intense interest as it may bridge the gap between optoelectronic devices and microelectronic circuits. Recently, InAs QDs-on-GaAs NW has been realized on Si substrate by Molecular Beam Epitaxy (MBE), which shows a good prospect in single photon sources [17]. In our previous work, it was shown that NW-based QDs grown by MOCVD typically have a large density. This means that the electron wave-functions may overlap with each other and results in an intermediate band, which makes the structure a promising candidate for novel QD intermediate band solar cells [18]. Apparently, integrating the III–V NW-based QDs on Si would have more appeal, e.g. a substantially reduced cost. However, so far there have been no reports of aforementioned structures on Si by MOCVD.

In this paper, we study the growth of InAs QDs-on-GaAs NW hybrid heterostructures on Si substrate by MOCVD. We show that the NW density and substrate surface can strongly affect the formation of QDs. By lowering the NW density, InAs QDs are realized with a short deposition time. A wetting layer of several nanometers is observed under the QD, indicating a Stranski–Krastanow (S–K) growth mode. The structural and optical properties of the QDs are studied in detail.

2. Experimental procedure

The growth was performed by using a Thomas Swan CCS-MOCVD system at a pressure of 100 Torr. Trimethylgallium (TMGa), trimethylaluminum (TMAl), trimethylindium (TMIn) and arsine were used as precursors. Au-catalyzed GaAs NWs were grown on Si (1 1 1) substrate by using AlGaAs/GaAs buffer layers, which was described in detail previously [19,20]. A difference is

* Corresponding author. Tel./fax: +86 10 6119 8040.
E-mail address: xzhang@bupt.edu.cn (X. Zhang).

0022-0248/$ - see front matter © 2013 Elsevier B.V. All rights reserved.
http://dx.doi.org/10.1016/j.jcrysgro.2013.09.014

that both Au film and Au colloidal particles were used to form Au–Ga alloy nanoparticles acting as catalyst, resulting in different NW densities. GaAs NWs were grown at 440 °C for 800 s, with a TMGa flow rate of 38.9 μmol min^{-1} and an AsH_3 flow rate of 2.87×10^{-3} mol min^{-1}. InAs QDs were then deposited at 475 °C with a TMIn flow rate of 11.3 μmol min^{-1} and a low AsH_3 flow rate of 71.8 μmol min^{-1}. The corresponding V/III ratio is 6.4. To study the optical properties of QDs, a GaAs capping shell with a thickness of about 20 nm was grown after the QDs. The temperature was kept at 475 °C for avoiding In desorption from the QDs. For comparison, aforementioned structures were also grown on GaAs (1 1 1) B substrate under same conditions.

Morphology and structure of the samples were characterized by Field Emission Scanning Electron Microscopy (FESEM) and Transmission Electron Microscopy (TEM), respectively. TEM specimens were prepared by ultrasonicating the samples in ethanol for 5 min, followed by spreading drops from the suspension onto a holey carbon/Cu grid. For optical characterization, as-grown NWs were mechanically cut down and dispersed onto a SiO_2-coated Si substrate. The microphotoluminescence (μPL) measurements were carried out using a 632.8 nm continuous-wave He–Ne laser for excitation. The excitation beam was focused onto ~2 μm in diameter with a × 50 microscope objective on the sample placed in a cryostat, with a power density of 16 kW cm^{-2}. The emission through the same microscope objective was detected by the combination of a grating spectrometer and a silicon charge-coupled device (CCD).

3. Results and discussion

Fig. 1 shows the SEM and TEM images of NWs on Si substrate with Au film as catalyst source. From Fig. 1(a), we can see that ultrahigh-density (estimated to be 1×10^{10} cm^{-2}) NW arrays are realized and most of NWs are vertical to the substrate. A 300 nm buffer layer can be identified clearly between the Si substrate and NWs, which is helpful to modifying the nonpolar nature of Si (1 1 1) surface and promoting the vertical growth [19]. After depositing 220 s of InAs, no QDs are observed on the NW surface, as shown in Fig. 1(b) and (c). Fig. 1(d) shows the high-resolution TEM (HRTEM) image of a single NW. A very thin layer (about 1.5 nm) can be seen on the edge of the NW, which is attributed to the InAs wetting layer. The growth rate of InAs is estimated to be 0.007 nm s^{-1}, which is much lower than that of InAs grown on GaAs-based GaAs NWs with the same flow rates (about 0.1 nm s^{-1}) [12]. The failure of QDs formation is mainly attributed to the high NW density. It has been demonstrated previously that QDs on Au-catalyzed NWs are mainly

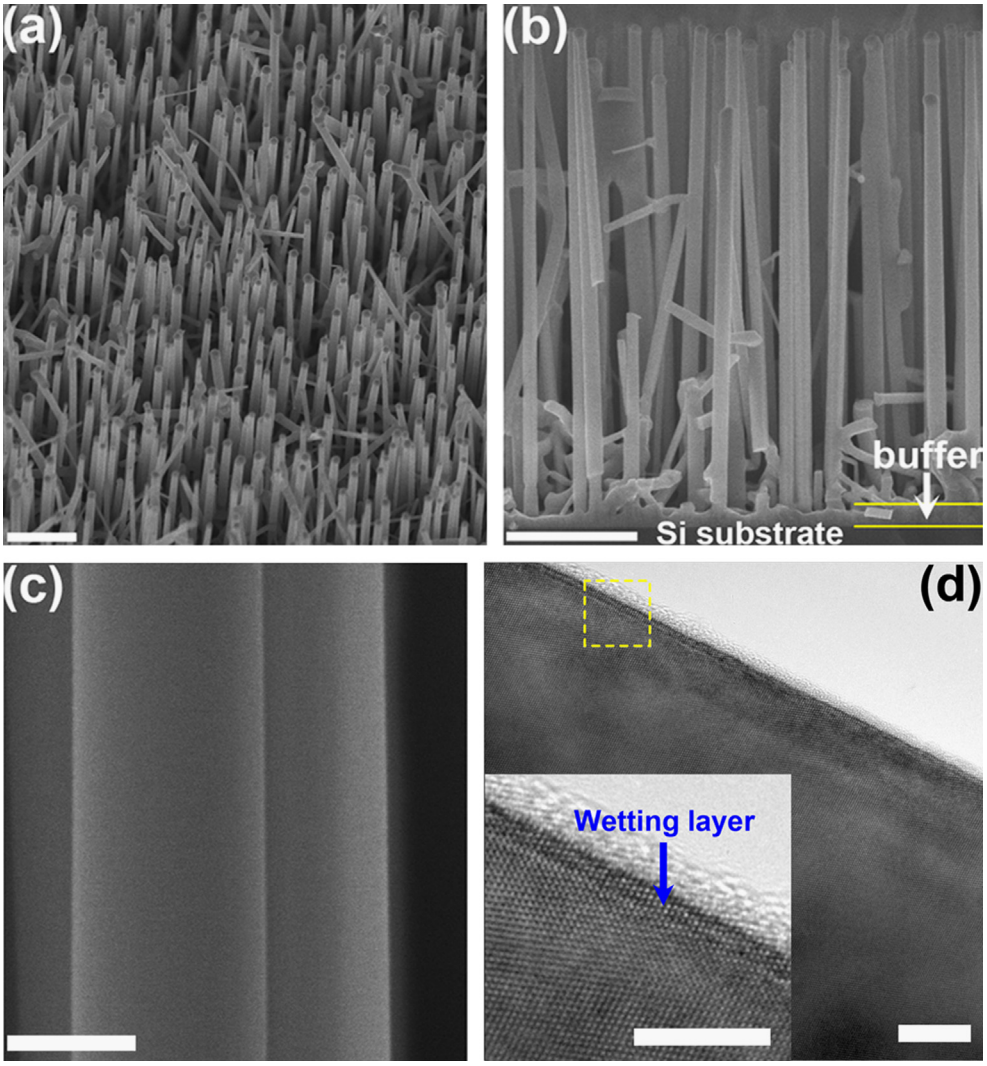

Fig. 1. SEM and TEM images of NWs on Si substrate with Au film as catalyst source. (a) Twenty degree tilted SEM image from the normal surface, (b) cross-sectional SEM image of NW arrays, (c) cross-sectional SEM image of a single NW, (d) HRTEM image of a single NW. The inset in (d) shows the enlarged HRTEM image of the wetting layer. Scale bars are 5 μm, 1 μm, 100 nm and 5 nm in (a), (b), (c) and (d), respectively.

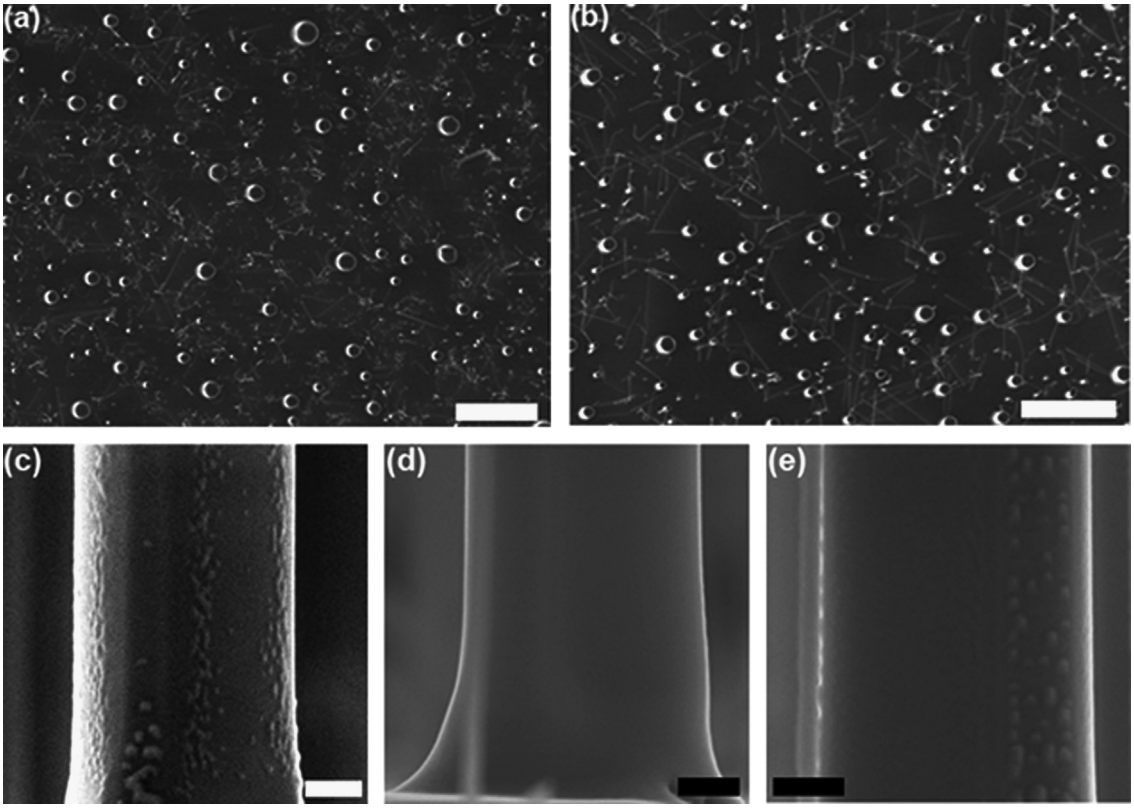

Fig. 2. (a) and (b) GaAs NW arrays from sample a (lower density) and sample b (higher density), respectively. (c) InAs-on-GaAs NW structures based on sample a, with 30 s deposition of InAs. (d), (e) InAs-on-GaAs NW structures based on sample b, with 30 s and 70 s deposition of InAs, respectively. Scale bars in (a) and (b) are 5 μm, in (c)–(e) are 100 nm.

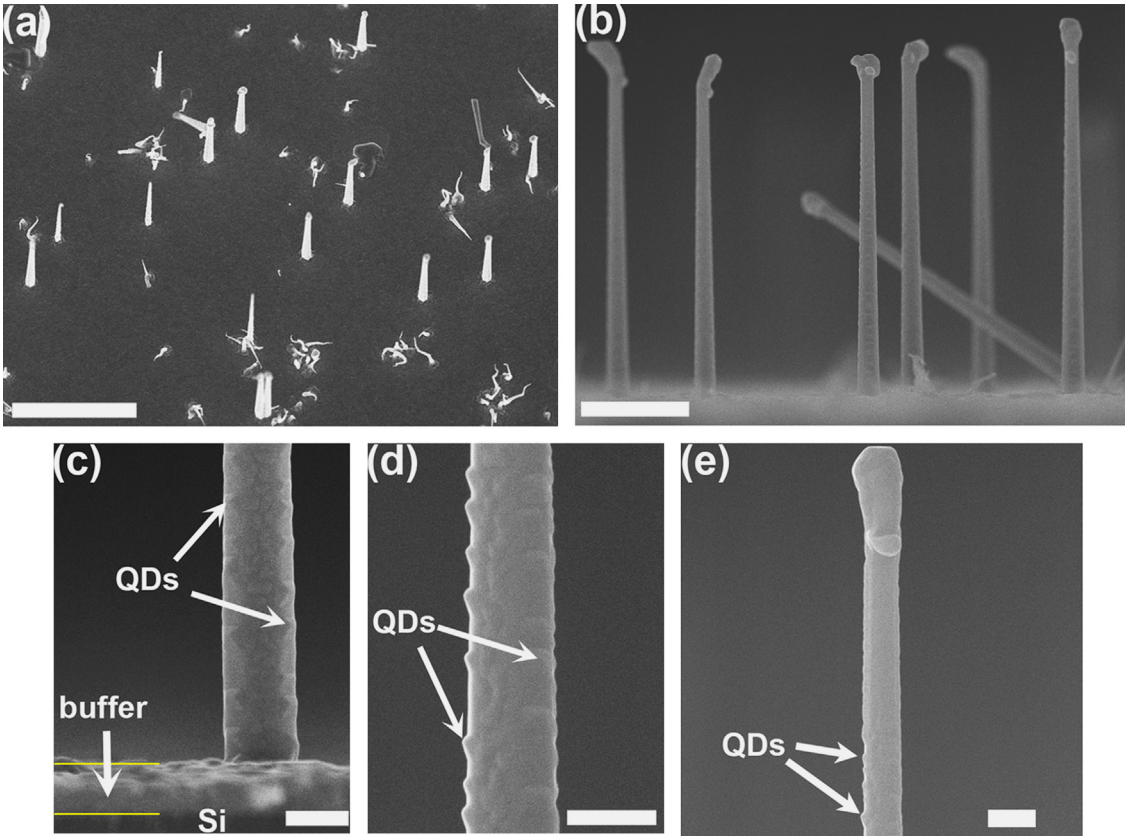

Fig. 3. SEM images of NWs on Si substrate with Au colloidal particles as catalyst source. (a) Twenty degree tilted image from the normal surface, (b) cross-sectional image, (c) cross-sectional image of a NW bottom, (d) cross-sectional image of a NW middle part and (e) cross-sectional image of a NW top. The scale bar in (a) is 5 μm, in (b) is 1 μm and in (c)–(f) is 100 nm.

formed by adatom diffusion from the substrate surface, which means that the In atoms first impinge on substrate and then diffuse to the NW sidewalls [15]. The high-density NW arrays dramatically prevent the precursors from being transported to the substrate. In addition, adjacent NWs may compete for adatoms as the distance between them (less than 1 μm) is much shorter than the In diffusion length on GaAs (1 1 1) B surface [20]. Both the two mechanisms can reduce the number of In adatoms contributing to the QDs formation.

To further demonstrate the effect of NW density on the formation of QDs, we study several InAs-on-GaAs NW structures on GaAs (111) B substrate with different NW densities by using Au films with different thickness as catalyst source. Fig. 2(a) and (b) show the top view SEM images of GaAs NW arrays from sample a and b, whose density is estimated to be $2.0\times10^7\ \mathrm{cm}^{-2}$ and $4.0\times10^7\ \mathrm{cm}^{-2}$, respectively. Fig. 2(c) shows a single InAs-on-GaAs NW based on sample a, with 30 s deposition of InAs. We can clearly find a lot of QDs on the NW surface. While in Fig. 2(d), no QDs are observed on the NW based on sample b, with a same deposition time of InAs. An equal number of QDs have not been observed until the deposition time is increased to 70 s, as shown in Fig. 2(e). It should be noted that the diameters are nearly the same in (c)–(e), which means that the effect of diameter on the formation of QDs can be ruled out [12]. Thus the difference can only be attributed to different NW densities, which supports our conclusion mentioned above.

Based on the discussions above, it is possible to grow InAs QDs on GaAs NWs grown on Si substrate by reducing the NW density. However, unlike that on GaAs substrate, NWs on buffer layer-coated Si substrate using Au film as catalyst source typically have a large density, possibly due to different surface properties. Alternatively, Au colloidal particles are used as catalyst source. Fig. 3 shows the corresponding SEM images, and we can see that most of the NWs are vertical to the Si substrate, with a much lower density of $5\times10^6\ \mathrm{cm}^{-2}$. The GaAs NWs exhibit a little taper, indicating stronger species diffusion from the sidewalls and substrate surface to the top due to low NW density [20]. By depositing InAs for a short time of 30 s, the NWs are nearly fully covered by several arrays of QDs from the bottom up, as shown in Fig. 3(b)–(e). The growth rate of InAs is estimate to be $0.2\ \mathrm{nm\ s}^{-1}$. This indicates that low NW density can dramatically enhance the impingement of precursors on the substrate as well as reduce the competition between neighbor nanowires. No QDs are observed on the top part of the NW near the Au particle, which is probably due to a limited diffusion length of In adatoms along the NW, as well as a collection of In adatoms by the Au particle [15,21].

Fig. 4 shows the SEM images of InAs QDs-on-GaAs NWs on GaAs (1 1 1) B substrate by using Au colloidal particles as catalyst source. The growth conditions are completely the same with that on Si substrate just mentioned. We find that the QDs have a higher density (12.8/μm/side facet) than that on Si (6.6/μm/side facet), which is attributed to different substrate surface properties. From Fig. 3(c) we can see that the surface of buffer layer on Si is rough and contains a lot of high-index surfaces, which is favorable for the incorporation of In adatoms [22]. Moreover, the roughness also

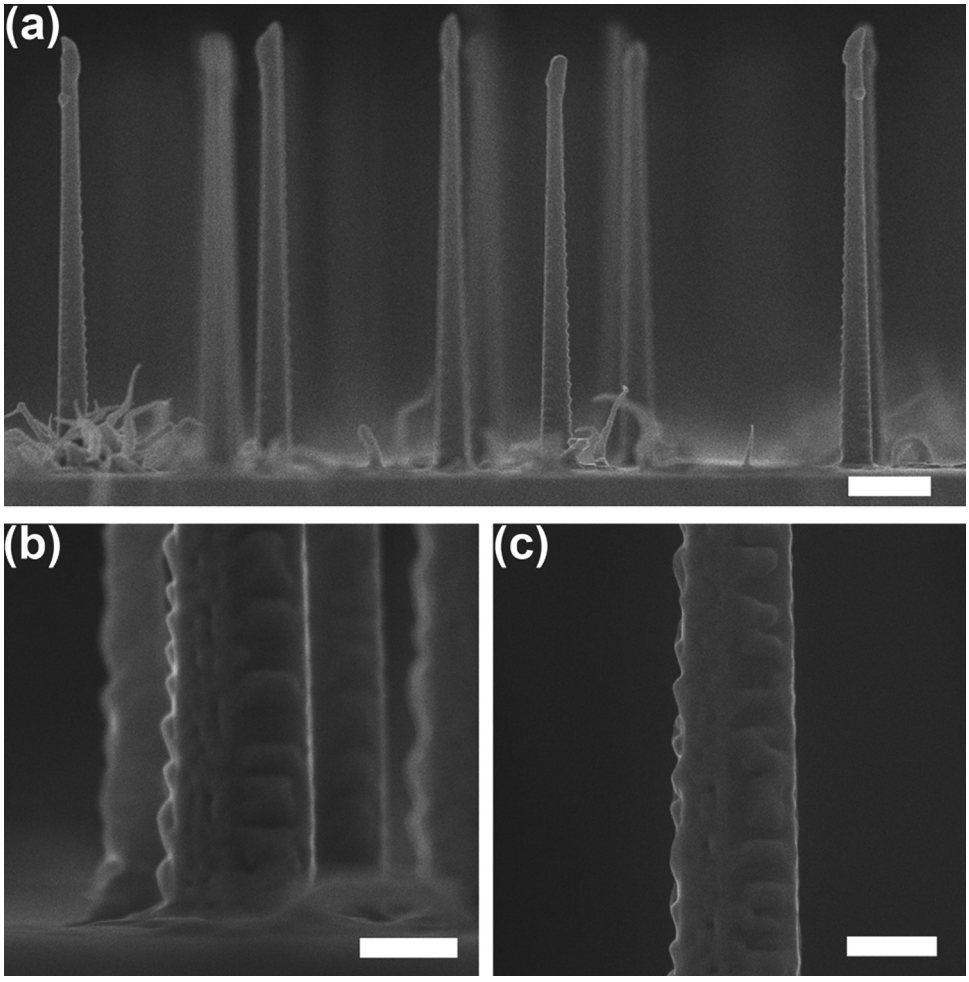

Fig. 4. SEM images of NWs on GaAs substrate with Au colloidal particles as catalyst source. (a) cross-sectional images of NWs, (b) cross-sectional image of a NW bottom and (c) cross-sectional image of a NW middle part. The scale bar in (a) is 1 μm, in (b) and (c) is 100 nm.

increases the surface area, which further enhances the In adatom absorption.

Based on the discussions above, we can conclude that the formation of NW-based QDs is more complicated than that on planar substrates as it is intimately associated with the NW density as well as the substrate surface properties, as both can strongly affect the surface diffusion. Thus, this offers us more roads to control the properties of QDs for various applications.

To investigate the crystal structure and surface faceting of QDs, TEM was conducted. Fig. 4(a) shows a single NW with a diameter decreasing from 225 to 145 nm from base to top. A thin layer with a thickness of 2–3 nm can be observed distinctly from Fig. 4(b), which is attributed to the InAs wetting layer. This is the first time that wetting layer is observed in InAs/GaAs QDs-on-NW structures, which offers a direct evidence for the Stranski–Krastanow (S–K) growth mode of InAs QDs on GaAs NW. The wetting layer thickness here is much larger than that on planar GaAs (1 0 0) substrate, which may be attributed to two mechanisms [23]. First, due to the small dimension, NW can share more strain energy caused by the lattice mismatch [24]. Second, the nanosized curve surface of the NW could also help to release the lattice strain [25]. Both the two mechanisms reduce the strain stored in the epitaxial layer and lead to a thicker wetting layer.

The shape, size and crystal structure of QDs were determined by HRTEM together with high-magnification top-view SEM. Fig. 4 (c) shows the HRTEM image of a single QD. Three facets are determined as $(1\ \bar{1}\ \bar{1})$, $(1\ 1\ \bar{2})$ and (1 1 0). Fig. 4(d) shows the high-magnification top-view SEM of a single QD. The remaining two surfaces are determined as $(0\ 1\ \bar{1})$ and $(1\ 0\ \bar{1})$. These facets are also observed in InAs QDs formed on planar GaAs (1 0 0) substrate [26,27]. Based on the above results, the general shape of the QDs is obtained, which is helpful to modeling the strain, electronic structures and other characteristics for further study. The side length of the QD bottom is estimated to be 30 nm while the height of the QD is about 10 nm. The QD exhibits high crystal quality, with pure ZB structure and very few dislocations. Fig. 5

PL characteristics of the samples are shown in Fig. 6. Fig. 6 (a) shows the 77 K PL spectra of NW with InAs QDs on GaAs and Si

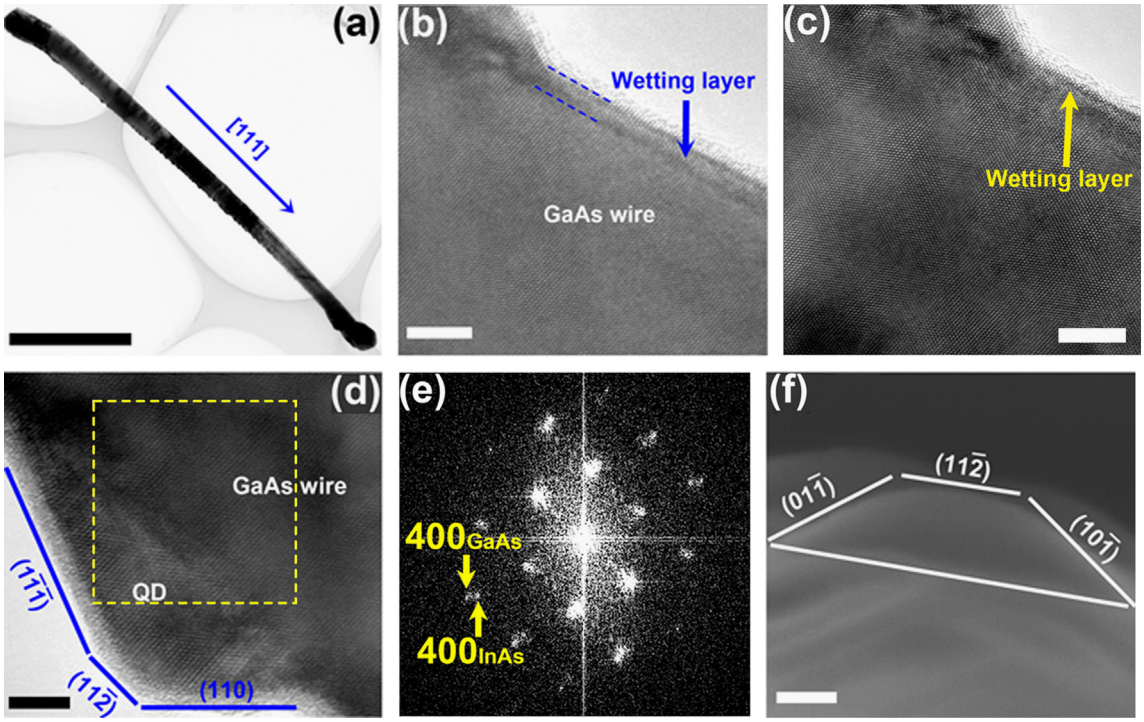

Fig. 5. (a) TEM image of a single NW with QDs, (b) TEM image of the wetting layer with QDs, (c) HRTEM image of the wetting layer, (d) HRTEM image of a single QD, (e) FFT of the square area in (d) and (f) top-view SEM image of a single QD. The scale bar in (a) is 1 μm while in (b)–(d) and (f) is 5 nm.

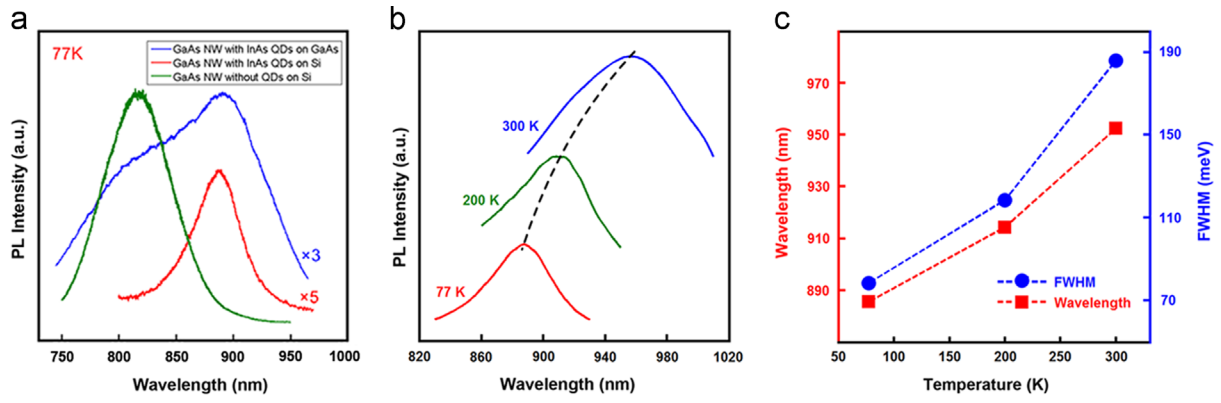

Fig. 6. (a) PL spectra of GaAs NW with InAs QDs on GaAs, on Si and GaAs NW without InAs QDs on Si, (b) Temperature-dependent PL spectra of InAs QDs on Si-based GaAs NWs and (c) temperature-dependent wavelength and linewidth of QDs.

substrates, as well as NW without QDs on Si. Only one emission peak is observed from the NW without QDs, which is attributed to the GaAs NW. No emission is detected from the InAs wetting layer, probably because that the emission from the thin wetting layer is very weak at 77 K. The InAs QDs grown on GaAs and Si substrates shows an emission with a similar peak wavelength at 885 nm. The wavelength is much shorter compared with the InAs QDs grown on planar GaAs substrate, which is attributed to the intermixing of QDs with GaAs NW as well as GaAs capping layer [28,29]. Due to the different surface properties between {1 1 2} and {0 0 1}, the intermixing of QDs with GaAs NW and capping layer may be more serious than that of QDs with {0 0 1} GaAs. The PL intensity of QDs grown on GaAs is stronger than that on Si, indicating a higher density of QDs grown on GaAs, which is consistent with the results in Figs. 3 and 4. Correspondingly, the linewidth of QDs grown on GaAs is also larger than that on Si, suggesting a broader size distribution of QDs. Fig. 6(b) and (c) show the temperature-dependent PL characteristics of the QDs grown on Si substrates. We can see that both the wavelength and linewidth of QDs increases with temperature. At room temperature, the emission is centered at 952 nm, with a broad linewidth of 186 meV. Compared with the emission from InAs QDs on GaAs NWs grown on GaAs substrate by using Au film as catalyst [12], the linewidth is much larger. A possible explanation is that the size distribution of QDs may be broader due to tapered geometry of the NW, much lower NW density or other unclear reasons which still need further investigations.

4. Summary

In summary, we have grown InAs/GaAs QDs-on-NW hybrid heterostructures on low-cost Si substrate by MOCVD. It is shown that the formation of QDs is strongly affected by the NW density as well as the substrate surface properties, which is more complicated than traditional QDs on planar substrates. Due to the large density and high quality of the QDs, this structure is promising in low-cost NW-based QD intermediate band solar cells. Moreover, the geometry of NWs also allows growing multi-layer QDs around the sidewalls and forming a 3D QD array, which may further improve the performance by enhancing the overlap of electron wavefunctions as well as increasing the number of QDs [30].

Acknowledgements

This work was supported by the National Basic Research Program of China (2010CB327600), the National Natural Science Foundation of China (61020106007, 61077049, 61211120195 and 61376019), the International Science & Technology Cooperation Program of China (2011DFR11010), the Specialized Research Fund for the Doctoral Program of Higher Education (20120005110011), the 111 Program of China (B07005) and BUPT Excellent Ph.D. Students Foundation (CX201213).

References

[1] F. Qian, Y. Li, S. Gradečak, H. Park, Y. Dong, Y. Ding, Z.L. Wang, C.M. Lieber, InP nanowire array solar cells achieving 13.8% efficiency by exceeding the ray optics limit, Nature Materials 7 (2008) 701.
[2] J. Wallentin, N. Anttu, D. Asoli, M. Huffman, I. Åberg, M.H. Magnusson, G. Siefer, P. Fuss-Kailuweit, F. Dimroth, B. Witzigmann, H.Q. Xu, L. Samuelson, K. Deppert, M.T. Borgström, InP nanowire array solar cells achieving 13.8% efficiency by exceeding the ray optics limit, Science 339 (2013) 1057.
[3] A.C. Scofield, A. Lin, J.N. Shapiro, P.N. Senanayake, G. Mariani, M. Haddad, B.L. Liang, D.L. Huffaker, Composite axial/core-shell nanopillar light-emitting diodes at 1.3 μm, Applied Physics Letters 101 (2012) 053111.
[4] M.S. Gudiksen, L.J. Lauhon, J. Wang, D.C. Smith, C.M. Lieber, Growth of nanowire superlattice structures for nanoscale photonics and electronics, Nature 415 (2002) 617.
[5] V.I. Klimov, A.A. Mikhailovsky, S. Xu, A. Malko, J.A. Hollingsworth, C. A. Leatherdale, H.-J. Eisler, M.G. Bawendi, Optical gain and stimulated emission in nanocrystal quantum dots, Science 290 (2000) 314.
[6] Y. Ding, J. Motohisa, B. Hua, S. Hara, T. Fukui, Observation of Microcavity Modes and Waveguides in InP Nanowires Fabricated by Selective-Area Metalorganic Vapor-Phase Epitaxy, Nano Letters 7 (2007) 3598.
[7] N. Panev, A.I. Persson, N. Sköld, L. Samuelson, Sharp exciton emission from single InAs quantum dots in GaAs nanowires, Applied Physics Letters 83 (2003) 2238.
[8] J. Claudon, J. Bleuse, N.S. Malik, M. Bazin, P. Jaffrennou, N. Gregersen, C. Sauvan, P. Lalanne, J. Gérard, Nature Photonics 4 (2010) 174.
[9] E. Uccelli, J. Arbiol, J.R. Morante, A.F. Morral, ACS Nano 4 (2010) 5985.
[10] K. Kawaguchi, M. Heurlin, D. Lindgren, M.T. Borgström, M. Ek, L. Samuelson, Applied Physics Letters 99 (2011) 131915.
[11] D. Lindgren, K. Kawaguchi, M. Heurlin, M.T. Borgström, M. Pistol., L. Samuelson, A. Gustafsson, Nanotechnology 24 (2013) 225203.
[12] X. Yan, X. Zhang, X. Ren, X. Lv, J. Li, Q. Wang, S. Cai, Y. Huang, Nano Letters 12 (2012) 1851.
[13] L. Pan, K. Lew, J.M. Redwing, E.C. Dickey, Nano Letters 5 (2005) 1081.
[14] D.G. Ramlan, S.J. May, J. Zheng, J.E. Allen, B.W. Wessels, L.J. Lauhon, Nano Letters 6 (2006) 50.
[15] X. Yan, X. Zhang, X. Ren, H. Huang, J. Guo, X. Guo, M. Liu, Q. Wang, S. Cai, Y. Huang, Nano Letters 11 (2011) 3941.
[16] X. Yan, X. Zhang, X. Ren, J. Li, X. Lv, Q. Wang, Y. Huang, Growth and photoluminescence of $In_xGa_{1-x}As$ quantum dots on the surface of GaAs nanowires by metal organic chemical vapor deposition, Applied Physics Letters 101 (2012) 023106.
[17] Y. Yu, M.F. Li, J.F. He, Y.M. He, Y.J. Wei, Y. He, G.W. Zha, X.J. Shang, J. Wang, L.J. Wang, G.W. Wang, H.Q. Ni, C.Y. Lu, Z.C. Niu, Single InAs Quantum Dot Grown at the Junction of Branched Gold-Free GaAs Nanowire, Nano Letters 13 (2013) 1399.
[18] A. Martí, N. López, E. Antolín, E. Cánovas, C. Stanley, C. Farmer, L. Cuadra, A. Luque, Novel semiconductor solar cell structures: The quantum dot intermediate band solar cell, Thin Solid Films 511–512 (2006) 638.
[19] H. Huang, X. Ren, X. Ye, J. Guo, Q. Wang, Y. Yang, S. Cai, Y. Huang, Growth of Stacking-Faults-Free Zinc Blende GaAs Nanowires on Si Substrate by Using AlGaAs/GaAs Buffer Layers, Nano Letters 10 (2010) 64.
[20] Y. Kim, H.J. Joyce, Q. Gao, H.H. Tan, C. Jagadish, M. Paladugu, J. Zou, A.A. Suvorova, Influence of nanowire density on the shape and optical properties of ternary InGaAs nanowires, Nano Letters 6 (2006) 599.
[21] W. Seifert, M. Borgström, K. Deppert, K.A. Dick, J. Johansson, M.W. Larsson, T. Mårtensson, N. Sköld, C.P.T. Svensson, B.A. Wacaser, L.R. Wallenberg, L. Samuelson, Growth of one-dimensional nanostructures in MOVPE, Journal of Crystal Growth 272 (2004) 211.
[22] M. Paladugu, J. Zou, Y. Guo, X. Zhang, H.J. Joyce, Q. Gao, H.H. Tan, C. Jagadish, Y. Kim, Formation of hierarchical InAs nanoring/GaAs nanowire heterostructures, Angewandte Chemie International Edition 48 (2009) 780.
[23] D. Leonard, K. Pond, P.M. Petroff, Critical layer thickness for self-assembled InAs islands on GaAs, Physical Review B: Condensed Matter 15 (1994) 11687.
[24] S. Raychaudhuri, E.Y. Yu, Critical dimensions in coherently strained coaxial nanowire heterostructures, Journal of Applied Physics 99 (2006) 114308.
[25] X. Li, G. Yang, Strain Self-Releasing Mechanism in Heteroepitaxy on Nanowires, Journal of Physical Chemistry C 113 (2009) 12402.
[26] M.C. Xu, Y. Temko, T. Suzuki, K. Jacobi, Shape transition of InAs quantum dots on GaAs (001), Journal of Applied Physics 98 (2005) 083525.
[27] J. Márquez, L. Geelhaar, K. Jacobi, Atomically resolved structure of InAs quantum dots, Applied Physics Letters 16 (2001) 2309.
[28] Ch. Heyn, A. Bolz, T. Maltezopoulos, R.L. Johnson, W. Hansen, Intermixing in self-assembled InAs quantum dot formation, Journal of Crystal Growth 278 (2005) 46.
[29] J. Lee, H. Ren, S. Sugou, Y. Masumoto, InGaAs quantum dot intermixing and evaporation in GaAs capping layer growth, Journal of Applied Physics 84 (1998) 6686.
[30] T. Sugaya, S. Furue, H. Komaki, T. Amano, M. Mori, K. Komori, S. Niki, O. Numakami, Y. Okano, Highly stacked and well-aligned InGaAs quantum dot solar cells with InGaAs cap layer, Applied Physics Letters 97 (2010) 183104.